

THERMAL-MECHANICAL BUCKLING OF COMPOSITE PLATES FOR AEROSPACE APPLICATIONS

Javier Gutiérrez Álvarez¹ and Chiara Bisagni²

¹Aerospace Structures and Computational Mechanics, Faculty of Aerospace Engineering,
Delft University of Technology, Kluyverweg 1, 2629HS Delft, Netherlands
Email: j.gutierrezalvarez@tudelft.nl

²Aerospace Structures and Computational Mechanics, Faculty of Aerospace Engineering,
Delft University of Technology, Kluyverweg 1, 2629HS Delft, Netherlands
Email: c.bisagni@tudelft.nl

Keywords: thermal-mechanical buckling, composite materials, analytical formulation, supersonic aircraft.

Abstract

A closed-form solution is proposed for determining the buckling of composite plates under combined thermal-mechanical loading. The plates are subjected to a constant temperature increment, combined with applied displacement, while transversal in-plane expansion is restricted. The plates are studied using Von Kármán equations in combination with classical lamination theory, being the study limited to symmetric and balanced laminates. The problem is formulated in terms of in-plane displacement fields and solved using the Galerkin method. An analytical formula is obtained that relates critical temperatures to applied plate displacement. An example of a possible application is presented in the form of graph and is verified by finite element analysis. The obtained formula can be used during initial design for sensitivity analysis and optimization, and also for deriving specific buckling shapes.

1. Introduction

Thermal buckling has been a topic of research since the early stages of supersonic flight, when the focus was on structures made of metallic materials [1-3]. In the following decades, several research activities were conducted to investigate the thermal buckling of laminate composite materials. Among the papers available in literature are those of Whitney and Ashton [4], Tauchert [5], Meyers and Hyer [6], Nemeth [7] or Jones [8]. However, most studies analyse thermal buckling with restricted expansions: plate edges are kept straight and constant in length, i.e. the original dimensions of the panel remain unchanged. Such boundary conditions prevent the plates from the introduction of external mechanical loads, such as compression or shear. There are, however, a few cases where the authors consider load introduction, such as the study of Nemeth [9] for infinite plates.

Although in the last decade extensive analytical research has been done in the field of pure mechanical buckling [10-13], there are few studies that explore combined thermal-mechanical buckling, like the one of Jones [14] for metallic materials, or the study of Abdalla et al. [15] for the optimization of tailored thin laminate panels. Being thermal-mechanical buckling a basic load case in aeronautical structures, there is a clear need of compact formulas valid for initial design.

An analysis of flat, symmetric and balanced composite laminated plates is here presented, where expansions are fully constrained at two opposite edges while temperature increment is applied and mechanical load is introduced in the form of axial displacement. The obtained closed-form solution can be applied to composite structures of the new supersonic aircrafts.

2. Analytical Formulation

A rectangular plate of length a and width b is considered, as shown in Figure 1. The plane XY coincides with the mid-plane of the plate and the Z axis is perpendicular to this plane. The plate presents the boundary conditions reported in equations (Eq. 1):

$$\begin{aligned} \text{At } x = 0, a: \quad u^o &= \pm \Delta_x/2 & \text{At } y = 0, b: \quad u^o &= \textit{free} \\ v^o &= \textit{free} & v^o &= 0 \\ w^o &= 0 & w^o &= 0 \end{aligned} \quad (1)$$

where u^o , v^o , w^o are the displacements of the plate mid-plane in the respective X , Y and Z directions. The plate is subjected to length variation Δ_x along X axis. Cases of plate stretching are represented by positive values of Δ_x , while for cases of plate shortening Δ_x assumes negative values. The whole plate experiments a uniform temperature increment ΔT respect to a stress-free state of equilibrium. The plate is analysed by means of Von Kármán plate theory in combination with classical lamination theory.

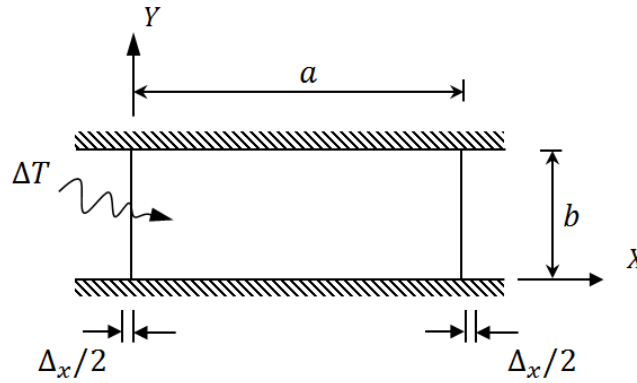


Figure 1. Composite plate subject to temperature and displacement.

The laminate stacking is assumed to be symmetric and balanced, and material properties are considered to remain constant within the analysed range of temperatures. The in-plane behaviour of the laminate is ruled by the membrane constitutive equation (Eq. 2):

$$\begin{Bmatrix} N_x \\ N_y \\ N_{xy} \end{Bmatrix} = \begin{bmatrix} A_{11} & A_{12} & 0 \\ A_{12} & A_{22} & 0 \\ 0 & 0 & A_{66} \end{bmatrix} \begin{Bmatrix} u_{,x}^o \\ v_{,y}^o \\ u_{,y}^o + v_{,x}^o \end{Bmatrix} - \begin{Bmatrix} N_x^T \\ N_y^T \\ N_{xy}^T \end{Bmatrix} \quad (2)$$

where N_x , N_y , N_{xy} are the force resultants at the plate edges, N_x^T , N_y^T , N_{xy}^T are the thermal force resultants, the terms A_{ij} , ($i, j = 1, 2, 6$) are the membrane stiffness terms from the classical lamination theory, and the comma followed by an index denotes differentiation with respect to that index. For homogeneous temperature distributions, the thermal force resultants can be expressed as in next equations (Eq. 3):

$$N_x^T = \hat{N}_x^T \Delta T \quad N_y^T = \hat{N}_y^T \Delta T \quad N_{xy}^T = \hat{N}_{xy}^T \Delta T \quad (3)$$

where \widehat{N}_x^T and \widehat{N}_y^T are the thermal force resultant per unit change of temperature. For symmetric and balanced laminates, \widehat{N}_{xy}^T vanishes and the remaining quantities assume the form given in presented equations (Eq. 4):

$$\widehat{N}_x^T = (A_{11}\alpha_x + A_{12}\alpha_y) \quad \widehat{N}_y^T = (A_{12}\alpha_x + A_{22}\alpha_y) \quad (4)$$

where α_x and α_y are the laminate expansion coefficients, as defined by Hyer [16]. The out-of-plane equilibrium equation can be expressed as in following equation (Eq. 5):

$$D_{11}w_{,xxxx} + 2(D_{12} + 2D_{66})w_{,xxyy} + D_{22}w_{,yyyy} - N_x w_{,xx} - N_y w_{,yy} = 0 \quad (5)$$

where the D_{ij} ($i, j = 1, 2, 6$) represent the laminate bending and twisting stiffness terms from the classical lamination theory. The in-plane displacement is described in linear function of the total variation of length Δ_x as in following equation (Eq. 6):

$$u^o = \frac{\Delta_x}{a}x - \frac{\Delta_x}{2} \quad (6)$$

while $v^o = 0$. The out-of-plane displacement can be expressed as a Fourier series as in following equation (Eq. 7):

$$w^o = \sum_{m=1}^{\infty} \sum_{n=1}^{\infty} W_{mn} \sin\left(\frac{m\pi x}{a}\right) \sin\left(\frac{n\pi y}{b}\right) \quad (7)$$

where W_{mn} is the amplitude of a generic Fourier coefficient, and m, n are the number of half waves for that particular series term in X and Y direction, respectively. The force resultants are determined by introducing the displacement field presented in Eq. 6 into the membrane constitutive relation (Eq. 2), yielding the following equations (Eq. 8):

$$N_x = A_{11} \frac{\Delta_x}{a} - \widehat{N}_x^T \Delta T \quad N_y = A_{12} \frac{\Delta_x}{a} - \widehat{N}_y^T \Delta T \quad (8)$$

After substituting Eq. 7 for the out-of-plane displacements and Eq. 8 for the force resultants into Eq. 5 for out-of-plane equilibrium, the following expression (Eq. 9) unfolds:

$$\sum_{m=1}^{\infty} \sum_{n=1}^{\infty} \left(\frac{\pi^4 (b^4 m^4 D_{11} + 2a^2 b^2 m^2 n^2 (D_{12} + 2D_{66}) + a^4 n^4 D_{22})}{a^4 b^4} + \frac{\pi^2 \left((a^2 n^2 A_{12} + b^2 m^2 A_{11}) \Delta_x - (\widehat{N}_x^T a b^2 m^2 + \widehat{N}_y^T a^3 n^2) \Delta T \right)}{a^3 b^2} \right) W_{mn} \sin\left(\frac{m\pi x}{a}\right) \sin\left(\frac{n\pi y}{b}\right) = 0 \quad (9)$$

The Galerkin method is based on the solution approximation of a differential equation by means of an assumed solution or trial function, here Eq. 7. Plugging this into Eq. 5 yields a residual which has to be minimized. This residual is given by the expression at the left of the equal sign in Eq. 9. The evaluation of the residual for a generic term of the Fourier series yields a generic equation, which is a function of a generic coefficient W_{mn} and the large bracket in Eq. 9. Equation solutions imply either W_{mn} being zero, also known as the trivial solution (i.e. the plate remains flat) or the content of the

bracket being zero. Solving the resulting equation with respect to ΔT , the following equation (Eq. 10) respect to ΔT is obtained:

$$\Delta T = \frac{a^2 n^2 A_{12} + b^2 m^2 A_{11} \left(\frac{\Delta_x}{a} \right)}{b^2 m^2 \hat{N}_x^T + a^2 n^2 \hat{N}_y^T} + \frac{\pi^2 (b^4 m^4 D_{11} + 2a^2 b^2 m^2 n^2 (D_{12} + 2D_{66}) + a^4 n^4 D_{22})}{a^2 b^2 (b^2 m^2 \hat{N}_x^T + a^2 n^2 \hat{N}_y^T)} \quad (10)$$

Eq. 10 represents states of equilibrium for which the out-of-plane deflections are nonzero. For each state of equilibrium given by the number of half-waves m and n , the obtained Eq. 10 relates plate length variations Δ_x with thermal increments ΔT . For a certain Δ_x , the buckling temperature is given by the configuration with the combination of m and n that delivers the lowest ΔT .

3. Application

An example is here presented in graphical form for a plate of dimensions $375 \text{ mm} \times 575 \text{ mm}$, made of AS4/3502 composite material, which properties are shown in Table 1. The plate has a quasi-isotropic sequence $[45/-45/0/90]_{25}$. The values of laminate expansion coefficients are $\alpha_x = \alpha_y = 1.72 \cdot 10^{-6} \text{ }^\circ\text{C}^{-1}$.

Table 1. AS4/3502 lamina properties.

E_{11} (MPa)	E_{22} (MPa)	G_{12} (MPa)	ν_{12}	$\alpha_1 \cdot 10^6$ ($^\circ\text{C}^{-1}$)	$\alpha_2 \cdot 10^6$ ($^\circ\text{C}^{-1}$)	t_{ply} (mm)
155000	8070	4550	0.22	-0.07	30.10	0.127

For the described plate a diagram of thermal increment ΔT versus applied length variation Δ_x is obtained from Eq. 10 and is reported in Figure 2.

Starting from a buckling shape with $m = 1, n = 1$ a line is obtained by plotting the resulting expression and is represented as dashed in the Figure. By leaving now $n = 1$ fixed and assuming $m = 1, 2, 3, \dots$ analogue dashed lines can be generated, being these lines related to buckling shapes with multiple half-waves in X direction. Repeating the operation with $m = 1, n = 1, 2, 3, \dots$ dashed lines related to buckling shapes with multiple half-waves in Y direction are reported.

Entering now Figure 2 with a given length variation Δ_x , the temperature at which the plate buckles is determined by the dashed line delivering the lowest value of ΔT . These lines intersect each other so the buckling shape defining the lowest ΔT will change depending on the mechanical loading condition Δ_x . The result of collecting all the lowest ΔT for any given Δ_x is the buckling curve, represented as bold in Figure 2, and is constituted by different segments of several intersecting dashed lines. The buckling curve divides the loading plane ($\Delta_x, \Delta T$) into two subspaces, corresponding to buckled and unbuckled states. The intersection of the buckling curve with the horizontal axis corresponds to the loading situation in which the plate buckles under pure mechanical loading ($\Delta T = 0 \text{ }^\circ\text{C}$); for this case, the length variation has a value of $\Delta_x = -0.04 \text{ mm}$ and the plate buckles under the shape of one half-wave in both X and Y directions. Conversely, the intersection with the vertical axis represents the case in which the plate remains constant in length ($\Delta_x = 0 \text{ mm}$) and buckles under pure heating. For this case, the thermal increment has a value of $\Delta T = 15.9 \text{ }^\circ\text{C}$, and the buckling shape has only one half-wave in both X and Y directions.

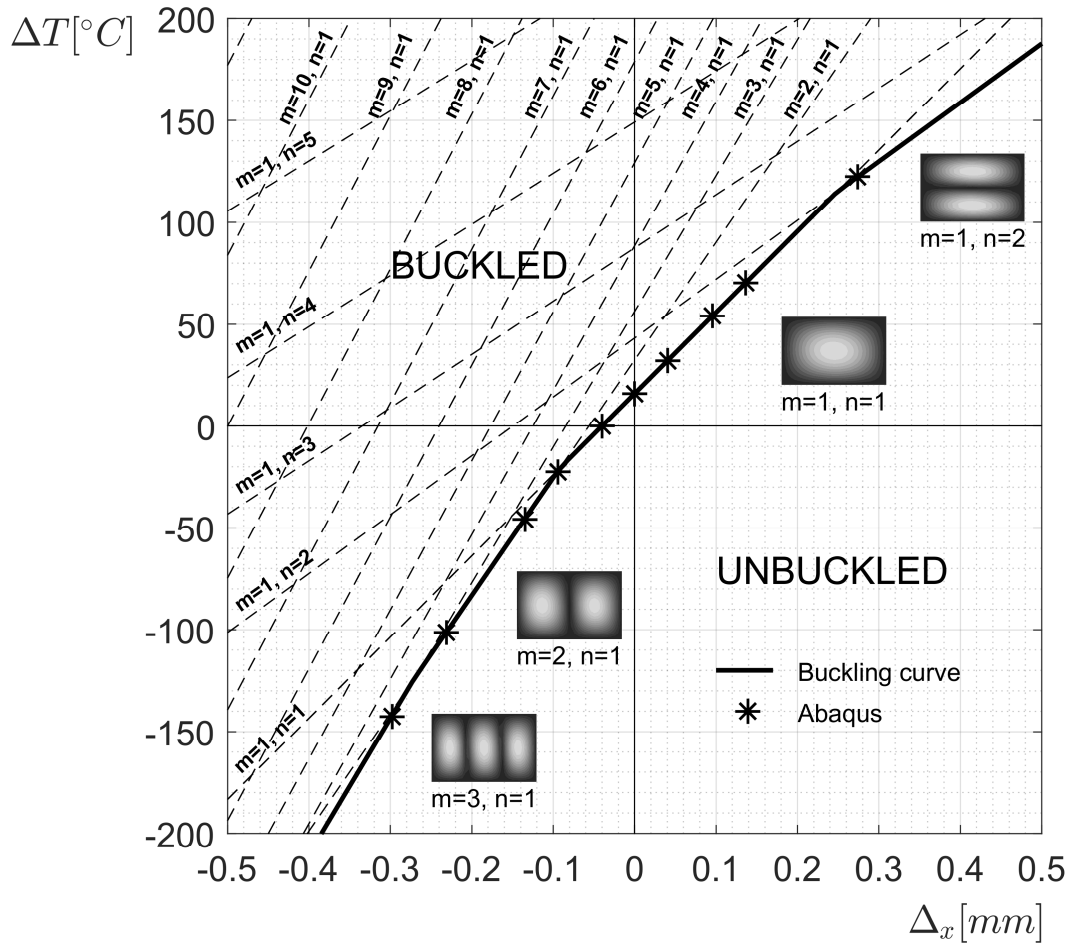


Figure 2. Buckling curve for thermal-mechanical buckling of composite plate.

If, for example, the plate experiments a stretch of $\Delta x = 0.3 \text{ mm}$, the buckling temperature increases significantly, rising up to $\Delta T = 129.9 \text{ }^\circ\text{C}$ and the buckling presents a mode with two half waves in Y direction. It is possible to note that under heating conditions, plate stretching has stabilizing effect against buckling. States of stretching and cooling induce biaxial tension states in the plate so buckling under this loading condition is not possible. Conversely, if the plate experiments a shortening of $\Delta x = -0.02 \text{ mm}$, buckling temperature descends to $\Delta T = 8.01 \text{ }^\circ\text{C}$. Under states of shortening and heating, the plate experiments a state of biaxial compression that noticeably reduces the buckling temperature.

Considering now a length variation of $\Delta x = -0.3 \text{ mm}$, the shortening is larger than the critical shortening for pure mechanical loading. In order to prevent the plate from buckling, it should be cooled down to temperatures lower than $\Delta T = -143.5 \text{ }^\circ\text{C}$; and the buckling pattern corresponds to three half-waves in the axial direction.

Finite element analysis were performed in Abaqus for verification. The plate is modelled with shell elements S4R, with element size of $20.8 \text{ mm} \times 20.5 \text{ mm}$. The plate is subjected to the boundary conditions described by the set of Eq. 1, and is loaded under combinations of mechanical load and temperature. The results of the eigenvalue analyses are reported in Figure 2 with the symbol of a star. Images of the buckling shapes obtained using Abaqus are also reported.

Figure 2 is restricted to a specific material, stacking and plate geometry, but similar figures can be generated for plates with different dimensions and materials by applying Eq. 10. These graphical results deliver valuable information for the initial phases of structural design. The deduced Expression (Eq. 10) can be readily implemented in optimization algorithms, allowing to obtain thermal-mechanical buckling with low computational effort. It can be also used for deriving targeted buckling shapes.

4. Conclusions

The combined thermal and mechanical buckling behaviour of thin, symmetric and balanced laminated plates was investigated. A formula was obtained, and a diagram illustrating the buckling behaviour of a rectangular plate was presented. The diagrams reports the buckling curve that divides the displacement-temperature loading space into two subspaces, corresponding to buckled and unbuckled states. It is shown how mechanically loaded laminated plates can be either stabilized or destabilized by either cooling or heating. The presented graph shows as well how buckling shapes can be achieved under particular loading conditions. The obtained results offer valuable insight for structural initial design. The deduced equation, due to its simplicity, can be used for sensitivity analysis and optimization.

References

- [1] N.J. Hoff. Thermal buckling of supersonic wing panels, *Journal of the Aeronautical Sciences*, 23:1019-1028, 1956.
- [2] K. Miura. Thermal buckling of rectangular plates. *Journal of the Aerospace Sciences*, 28:341-342, 1961.
- [3] E.A. Thornton. *Thermal Structures for Aerospace Applications*. AIAA, 1996.
- [4] J.M. Whitney and J.E. Ashton. Effect of environment on the elastic response of layered composite plates. *AIAA Journal*, 9:1708-1713, 1971.
- [5] T. R. Tauchert. Thermal buckling of thick antisymmetric angle-ply laminates. *Journal of Thermal Stresses*, 10:113-124, 1987.
- [6] C.A. Meyers and M.W. Hyer. Thermal buckling and postbuckling of symmetrically laminated composite plates. *Journal of Thermal Stresses*, 14:519-540, 1991.
- [7] M.P. Nemeth. Buckling behavior of long anisotropic plates subjected to fully restrained thermal expansion (TP-2003-212131). NASA Langley Research Center, 2003.
- [8] R.M. Jones. Thermal buckling of uniformly heated unidirectional and symmetric cross-ply laminated fiber-reinforced composite uniaxial in-plane restrained simply supported rectangular plates. *Composites Part A: Applied Science and Manufacturing*, 36:1355-1367, 2005.
- [9] M.P. Nemeth. Buckling behavior of long anisotropic plates subjected to restrained thermal expansion and mechanical loads. *Journal of Thermal Stresses*, 23:873-916, 2000.
- [10] R. Vescovini and C. Bisagni. Semi-analytical buckling analysis of omega stiffened panels under multi-axial loads. *Composite Structures*, 120:285-299, 2015.
- [11] C. Bisagni and R. Vescovini. Analytical formulation for local buckling and post-buckling analysis of stiffened laminated panels. *Thin-Walled Structures*, 47:318-334, 2009.
- [12] P.M. Weaver and M.P. Nemeth. Improved design formulas for buckling of orthotropic plates under combined loading. *AIAA Journal*, 46:2391-2396, 2008.
- [13] J.E. Herencia, P.M. Weaver and M.I. Friswell. Closed-form solutions for buckling of long anisotropic plates with various boundary conditions under axial compression. *Journal of Engineering Mechanics*, 136:1105-1114, 2010.
- [14] R.M. Jones. *Buckling of Bars, Plates, and Shells*. Bull Ridge Publishing, 2006.
- [15] M.M. Abdalla, Z. Gürdal and G.F. Abdelal. Thermomechanical response of variable stiffness composite panels. *Journal of Thermal Stresses*, 32:187-208, 2009.
- [16] M.W. Hyer. *Stress Analysis of Fiber-Reinforced Composite Materials*. Mc Graw-Hill, 1998.